Liquid Biopsy Enables Quantification of the Abundance and Interindividual Variability of Hepatic Enzymes and Transporters

Brahim Achour[1,*], Zubida M. Al-Majdoub[1], Agnieszka Grybos-Gajniak[2], Kristi Lea[3], Peter Kilford[4], Mian Zhang[4], David Knight[5], Jill Barber[1], Jeoffrey Schageman[3] and Amin Rostami-Hodjegan[1,6]

Variability in individual capacity for hepatic elimination of therapeutic drugs is well recognized and is associated with variable expression and activity of liver enzymes and transporters. Although genotyping offers some degree of stratification, there is often large variability within the same genotype. Direct measurement of protein expression is impractical due to limited access to tissue biopsies. Hence, determination of variability in hepatic drug metabolism and disposition using liquid biopsy (blood samples) is an attractive proposition during drug development and in clinical practice. This study used a multi-"omic" strategy to establish a liquid biopsy technology intended to assess hepatic capacity for metabolism and disposition in individual patients. Plasma exosomal analysis (n = 29) revealed expression of 533 pharmacologically relevant genes at the RNA level, with 147 genes showing evidence of expression at the protein level in matching liver tissue. Correction of exosomal RNA expression using a novel shedding factor improved correlation against liver protein expression for 97 liver-enriched genes. Strong correlation was demonstrated for 12 key drug-metabolizing enzymes and 4 drug transporters. The developed test allowed reliable patient stratification, and *in silico* trials demonstrated utility in adjusting drug dose to achieve similar drug exposure between patients with variable hepatic elimination. Accordingly, this approach can be applied in characterization of volunteers prior to enrollment in clinical trials and for patient stratification in clinical practice to achieve more precise individual dosing.

Study Highlights

WHAT IS THE CURRENT KNOWLEDGE ON THE TOPIC?

☑ Precision dosing aims to deliver the right dose of a drug to the right patient. This requires a diagnostic test to stratify patients according to their individual metabolic capacity. Implementation of patient stratification using genetics has not been successful.

WHAT QUESTION DID THIS STUDY ADDRESS?

☑ Can patients be stratified based on their individual hepatic elimination capacity using liquid biopsy? Can liquid biopsy input be used to design individualized dosage regimens for patients with variable hepatic elimination?

WHAT DOES THIS STUDY ADD TO OUR KNOWLEDGE?

☑ This study developed a pharmacological test based on liquid biopsy measurement to monitor hepatic expression levels of key enzymes and transporters. This allowed effective patient stratification and enabled improved precision of drug dose selection.

HOW MIGHT THIS CHANGE CLINICAL PHARMACOLOGY OR TRANSLATIONAL SCIENCE?

☑ This technology should facilitate patient stratification to achieve more precise dosing in the clinic and should enable improved characterization of volunteers prior to enrollment in clinical trials.

The liver has a central role in the metabolic elimination of not only endogenous compounds but also exogenous chemicals, including the majority of drugs. Variability in individual capacity for hepatic elimination of therapeutic drugs has been recognized and systematically studied over the past 50 years.[1] Differences between patients in response to drug therapy are therefore common and they represent a persistent challenge for clinicians, often leading to suboptimal patient care.[2] Departure from the "one-size-fits-all" approach to dosing, routinely practiced in the clinic, to more individualized therapy has been advocated by recent guidance,[3,4] with the objective of improving drug efficacy, reducing adverse reactions, and minimizing medicines wastage. In most cases, implementation of precise dosing has been linked to differences in genetics, particularly those affecting drug pharmacokinetics,[5]

[1]Centre for Applied Pharmacokinetic Research, School of Health Sciences, University of Manchester, Manchester, UK; [2]Illumina, Cambridge, UK; [3]Thermo Fisher Scientific, Austin, Texas, USA; [4]Simcyp Division, Certara Ltd., Sheffield, UK; [5]Biological Mass Spectrometry Core Facility, University of Manchester, Manchester, UK; [6]Certara Ltd., Princeton, New Jersey, USA. *Correspondence: Brahim Achour (brahim.achour@manchester.ac.uk)

Received July 17, 2020; accepted October 14, 2020. doi:10.1002/cpt.2102

such as polymorphisms in CYP2D6[6] and CYP2C9.[7] However, despite the important role of pharmacogenetics in determining drug pharmacology, there is evidence of large expression variability within each genotype,[6,8] which can only be captured by expression data, and there are no known genetic signatures that define the wide expression variations observed for certain key enzymes, such as CYP3A4.[9]

A survey of the contribution of specific enzyme families to drug metabolism showed that cytochrome P450 and glucuronosyltransferase enzymes mediate the direct metabolism of ~ 90% of the 200 most prescribed drugs in the United States in 2002,[10] a trend that changed very little in recent years.[11] The drug-eliminating function of the liver is also predicated on drug transporters, which play a key role in trafficking drugs and their metabolites in and out of liver cells. The interplay between the function of enzymes and transporters dictates a patient's exposure to a certain drug.[12] Guiding patient stratification and individual dosing will therefore crucially require quantitative characterization, beyond genetics, of hepatic enzymes and transporters in individual patients.[13] Access to tissue biopsies is limited,[14] and development of an effective and minimally invasive assay for patient stratification remains an essential requisite for precision dosing to become a clinical reality.[15]

In this study, we present a novel "liquid biopsy" test based on the analysis of enzymes and transporters in plasma exosomes isolated from individual blood samples. A quantitative link with protein expression in matching liver tissue was established, for the first time, by accounting for specific shedding of exosomes from the liver into the bloodstream. The utility of the test was demonstrated in relation to identifying patients at the extremes of drug exposure and guiding drug dose selection using an *in silico* model.

METHODS

Human plasma and liver samples

Matched blood and liver samples were collected with informed consent from 29 patients (16 men, age range 44–85 years) undergoing surgical resection for liver cancer at the Manchester Royal Infirmary, Manchester University NHS Foundation Trust, UK, and stored at the Manchester Biomedical Research Centre biobank. Ethical approval was granted by the North West Research Ethics Committee (14/NW/1260, 19/NW/0644). Liver samples were removed from histologically normal tissue adjacent to tumors. Blood was fractionated, and platelet-depleted plasma was stored in EDTA-treated cryogenic tubes at −80°C. Healthy (control) plasma from five donors (3 men, age range 23–57 years) was supplied by BioIVT (West Sussex, UK). One plasma sample was collected from each patient/donor; in the case of patients with cancer, collection was carried out within 1 hour prior to surgery. **Tables S1** and **S2** show demographic and clinical information for the 29 and 5 donors, respectively. The experimental workflow for tissue and plasma (liquid biopsy) processing is summarized in **Figure 1a**.

Exosomal RNA extraction and sequencing

Plasma exosome extraction was carried out using polymer-assisted precipitation (ExoQuick; System Biosciences, Palo Alto, CA), following the manufacturer's instructions. Exosomal pellets were reconstituted in 200 µl nuclease-free 1X phosphate-buffered saline, pH 7.4. Purity of exosomal preparations was not assessed; the presence of exosomes was confirmed by transmission electron microscopy using a Tecnai 12 Biotwin microscope (FEI Ltd., Cambridge, UK). Cell-free RNA (cfRNA) was extracted by MagMax cell-free total nucleic acid isolation kit (Thermo Fisher Scientific, Austin, TX), according to the manufacturer's protocol. Reverse transcription was performed with 3.5 µl of isolated cfRNA using AmpliSeq cDNA Synthesis for Illumina (Cambridge, UK). The cDNA (5 µl) was used in target amplification by polymerase chain reaction (16 cycles) using AmpliSeq Transcriptome Human Gene Expression Panel and AmpliSeq HiFi Mix (Illumina). Libraries were prepared for sequencing using AmpliSeq Library PLUS (96 reactions). Amplicon libraries were purified using Agencourt AMPure XP (Thermo Fisher Scientific) and further amplified (7 cycles). Universal primers complementary to adapter flow cell binding sites (P5 and P7) were used, and the final libraries were purified using Agencourt AMPure XP with size selection to remove fragments < 200 bp and > 700 bp. Normalized libraries (2 nM) were pooled and diluted (to 400 pM). Libraries were sequenced on NovaSeq 6000 platform (Illumina) with 2 × 150 bp paired-end reads using NovaSeq 6000 S2 Reagent kit (300 cycles). See **Supporting Methods** for additional details.

Sequencing data analysis was performed using RNA Amplicon App 2.0.1 (Illumina), alignment used the Burrows Wheeler Aligner and differential expression analysis used DESeq2.[16] Targets (enzymes/transporters) and liver-specific markers (used to describe shedding) were selected based on predefined criteria (**Table 1** and **Supporting Methods**). The selected markers were APOA2, FGB, AHSG, HPX, SERPINC1, F2, CFHR2, F9, SPP2, MBL2, A1BG, TF, and C9. Targets included cytochrome P450 enzymes (CYP1A2, 2A6, 2C9, 2C19, 2D6, 2E1, 3A4, and 3A5), glucuronosyltransferases (UGT1A1, 1A9, 2B4, and 2B7), and transporters (ABCB1, ABCG2, ABCC2, and SLCO1B1). A cutoff of > 3 reads per transcript was considered for quantification. Expression levels were recorded relative to the total number of reads in each sample as reads per million (RPM).

Normalization of RNA expression using liver-specific exosomal shedding

Expression levels in plasma exosomes combine variability in liver expression and variability in shedding from the liver into the bloodstream. To offset variability in shedding, a novel shedding factor (SF) was devised based on plasma RNA of liver-specific markers (**Table 1**). SF was calculated for each sample according to Equation 1, and target levels were normalized to patient-specific shedding using Equation 2.

$$\mathrm{SF}_j = \sum_{i=1}^{n} \left[\mathrm{cfRNA}\right]_{\mathrm{Marker}_{i,j}} / n \tag{1}$$

$$\mathrm{Normalized}\left[\mathrm{cfRNA}\right]_{\mathrm{Target}_{k,j}} = \left[\mathrm{cfRNA}\right]_{\mathrm{Target}_{k,j}} / \mathrm{SF}_j \tag{2}$$

SF_j (in RPM) is the shedding factor for sample j, $\left[\mathrm{cfRNA}\right]_{\mathrm{Marker}_{i,j}}$ represents cfRNA concentration (in RPM) of marker i in sample j relative to the total number of reads in sample j, and n is the number of markers used to construct the SF. $\left[\mathrm{cfRNA}\right]_{\mathrm{Target}_{k,j}}$ is cfRNA concentration of target k in sample j.

Proteomic analysis of liver samples

Liver tissue (42–379 mg) was mechanically homogenized, and membrane fractions were prepared by differential centrifugation at 10,000 *g* for 20 minutes, followed by 100,000 *g* for 75 minutes. Protein content of homogenates and fractions was measured with the Bradford assay. Recovery of reticular and plasma membrane was assessed using cytochrome P450 reductase (Sigma-Aldrich, Poole, UK) and alkaline phosphatase (Abcam, Cambridge, UK) assays, respectively. Individual samples and a quality control pool (43–50 µg protein) were prepared

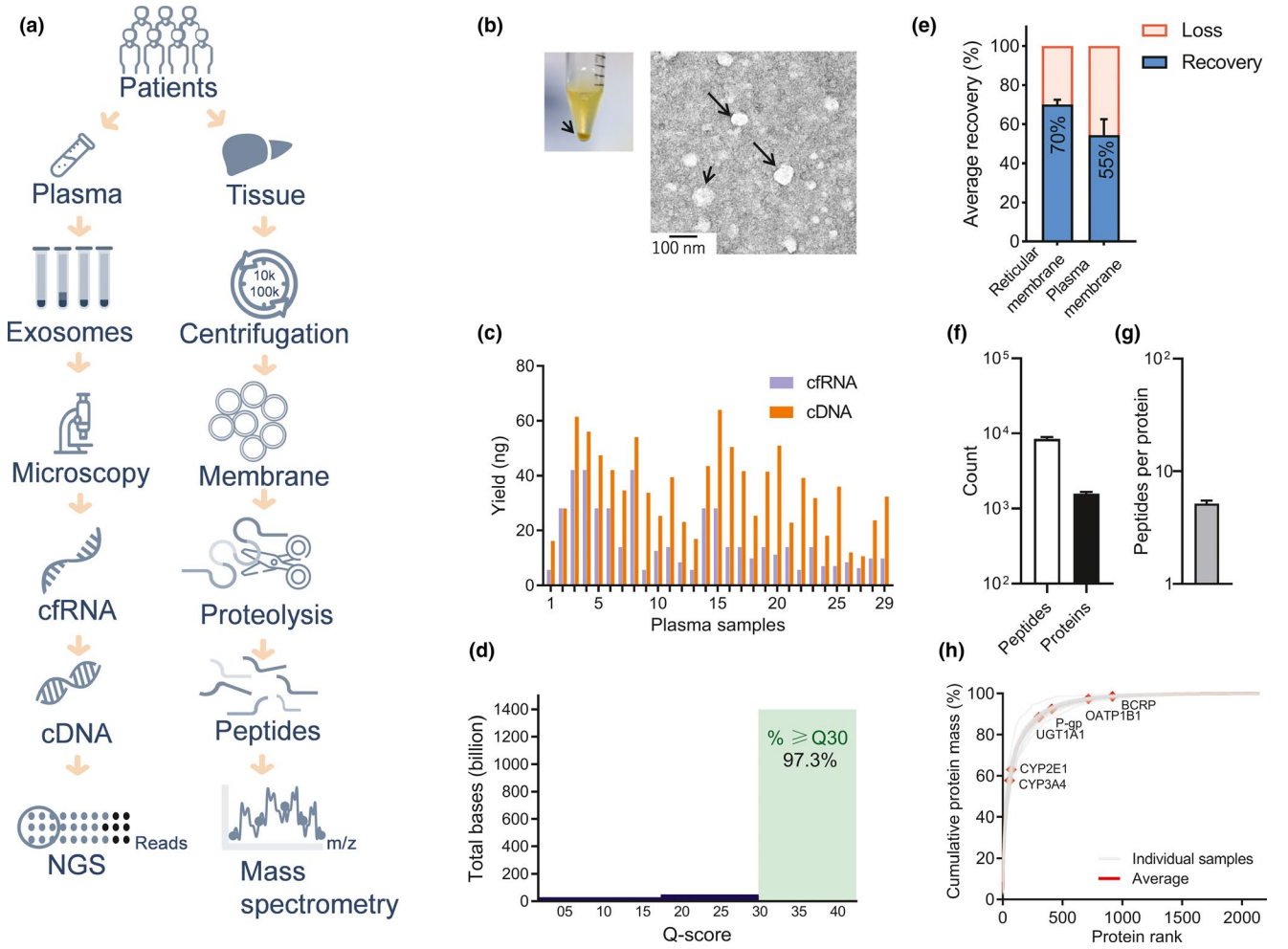

Figure 1 Multi-omic analysis of matched liver and plasma samples. (**a**) The experimental workflow started at collection of matched liver and blood samples from the same patients. Blood was fractionated to isolate plasma, followed by isolation of exosomes and extraction of cell-free RNA (cfRNA), which was analyzed by next generation sequencing (NGS). Tissue was homogenized and processed by differential centrifugation to extract membrane fractions, followed by proteolysis of membrane proteins and mass spectrometric analysis. (**b**) Exosomal pellets extracted from plasma by polymer-assisted precipitation were visually inspected and examined by transmission electron microscopy (×13,000). (**c**) The yields of cfRNA (from each sample) and corresponding reverse transcribed cDNA were assessed, which reflected variability between samples. (**d**) Sequencing quality was examined, reflecting high quality scores (Q-scores). (**e**) For tissue processing, the level of membrane recovery (mean ± SE of the mean) was assessed using resident markers of endoplasmic reticulum and plasma membranes. (**f**) Proteomic analysis by mass spectrometry generated peptide and protein data, reflecting consistently high numbers of identified peptides and on average similar numbers of proteins (mean ± SD). (**g**) Protein identification was carried out with a sufficient number of peptides per protein (mean ± SD). (**h**) Quantification of proteins was possible for 84% of identified proteins using global proteomic data (n = 2,143), spanning 5 orders of magnitude. Of these, targeted measurement of eight enzymes, four transferases, and four transporters was possible using signature peptide data relative to QconCAT standard; the rank order of key target proteins is shown.

for proteomics using filter-aided sample preparation,[17,18] with protein solubilization by sodium deoxycholate (10% w/v). Stable isotope-labelled MetCAT (5 µl) and TransCAT (9 µl)[19] were used as QconCAT standards for targeted proteomics. Disulfide bonds were reduced using 100 mM 1,4-dithiothreitol, followed by alkylation with 50 mM iodoacetamide. Proteolysis used LysC (2% w/w, 30°C, 3 hours) and trypsin (4% w/w, 37°C, 16 hours). Unlabeled peptides, EGVNDNEEGFFSAR and GVNDNEEGFFSAR, were added at 38 and 125 fmol, respectively, to quantify the QconCAT standards.[19,20] Samples were analyzed using an UltiMate 3000 rapid separation liquid chromatography system (Dionex, Surrey, UK) connected to an Orbitrap Elite mass spectrometer (Thermo Fisher Scientific, Waltham, MA). Chromatography was carried out over a 90-minute gradient and eluted peptides were analyzed over 350–1,500 mass-to-charge (m/z) range at resolution of 120,000 (at m/z 400). Data-dependent acquisition was used to select the top 10 multiply-charged (+ 2 and + 3) ions for fragmentation by collision-induced dissociation, either automatically or a preference list was applied (to select QconCAT[19] peptides).

Analysis and annotation of proteomic data

Proteomic data were processed using MaxQuant 1.6.7.0 (Max Planck Institute, Martinsried, Germany). Data were searched against a customized database, comprising human UniprotKB database (74,788 sequences) and two QconCAT sequences. For targeted analysis, data acquired with the preference list were searched for heavy and light QconCAT peptides. Light-to-heavy intensity ratios were applied with QconCAT concentrations to calculate protein levels, as previously described.[20] For global proteomic analysis, data collected using default

Table 1 Criteria for selecting liver markers and targets measured in plasma exosomes

Markers				Targets			
Marker	Tissue specificity (fold)[a]	Liver expression[b]	Detection in plasma (%)[c]	Target	Tissue specificity (fold)[a,d]	Detection in plasma (%)[c]	RNA-protein correlation in tissue[e]
APOA2	Liver (1068)	++++	100	CYP3A4	Liver (45)	97	Yes
FGB	Liver (556)	++++	100	CYP2D6	Liver (7)	83	Yes
AHSG	Liver (1903)	+++	100	CYP2C9	Liver (5)	100	Yes
				CYP1A2	Liver (31)	97	Yes
HPX	Liver (506)	+++	90	CYP2A6	Liver (165)	93	Yes
SERPINC1	Liver (670)	+++	93	CYP2C19	Liver (16)	97	Yes
F2	Liver (1472)	+++	93	CYP2E1	Liver (87)	100	Yes
				CYP3A5	Liver, intestine	76	Yes
CFHR2	Liver (4661)	+++	100	UGT1A1	Liver (16)	83	Yes
F9	Liver (2258)	+++	93	UGT1A9	Liver, kidney	48	–[f]
SPP2	Liver (2145)	++	79	UGT2B4	Liver (105)	97	–[f]
MBL2	Liver (1414)	++	76	UGT2B7	Liver (5)	76	–[f]
A1BG	Liver (180)	++	90	P-gp	Liver, intestine	100	Yes
				MRP2	Liver (3)	90	Yes
TF	Liver (12)	++	97	BCRP	Liver, intestine	100	Yes
C9	Liver (577)	++	83	OATP1B1	Liver (618)	93	Yes

Liver-specific markers were used to calculate variability in shedding from the liver to the bloodstream. The markers were liver-specific, highly expressed in liver tissue, and consistently detectable in plasma. Targets were key drug-metabolizing enzymes and drug transporters, predominantly expressed in the liver (and released into the blood), detectable in plasma, preferably with evidence of correlation between RNA and protein in liver tissue.
[a]Evidence from the Human Protein Atlas (HPA)[28]; the tissue specificity score is defined as fold difference relative to the organ with the second highest expression. [b]Evidence from the HPA.[28] [c]Proportion of plasma samples (n = 29) in which a marker/target was detected. [d]Targets are expressed in the liver and shedding is predominantly into the bloodstream. [e]Evidence of RNA-protein correlation in tissue from in-house and literature data. See **Table S10**. [f]Lack of evidence from previous studies for RNA-protein correlation in tissue.

acquisition settings were processed using the total protein approach.[21] Target concentrations were converted to tissue levels by multiplying by total protein content per unit tissue mass. Proteins identified by global proteomics were annotated for subcellular location (using Uniprot[22] and Gene Ontology)[23] and molecular function (using Protein Analysis THrough Evolutionary Relationships (PANTHER)[24] and the Database for Annotation, Visualization, and Integrated Discovery (DAVID)).[25]

In silico trials for dose selection using liquid biopsy

Quantitative multi-omic data were used to establish a quantitative link between plasma exosomal and liver tissue expression. To simulate the impact of liquid biopsy input on dose selection, drug trials were performed using Simcyp 18 release 2 (Sheffield, UK). Three CYP3A substrates were evaluated: alprazolam (low hepatic clearance), midazolam (medium clearance), and ibrutinib (high clearance). Compound files were selected from the Simcyp library. Key parameters were those accessible from patient information or a blood sample in a routine clinical trial (**Table S11**). Three scenarios were simulated as follows (**Table S12**).

1. Uniform dosing: virtual individuals were administered a uniform oral dose, as detailed in routine prescribing information (0.5 mg alprazolam, 5 mg midazolam, or 140 mg ibrutinib).
2. Stratified dosing: the same population was stratified into three groups based on their hepatic CYP3A4 content (liquid biopsy input). Simulations did not account for intestinal CYP3A4. For midazolam and ibrutinib, the top quartile was administered a dose twofold higher than the standard dose; the bottom quartile was administered a dose threefold lower. For alprazolam, a twofold dose increase for the top quartile and a twofold dose reduction for the bottom quartile were made. Dose selection for the two quartiles was guided by expression levels and the outcome of the uniform dosing simulation. The middle group (the remaining 50% of the population) were administered a standard dose.
3. Individualized dosing: the same individuals were administered a dose based on the ratio of their individual hepatic CYP3A4 content to the population average to simulate individual liquid biopsy input.

Drug exposure was measured as the area under the curve (AUC) of the plasma concentration-time profile, and population variability was calculated as coefficient of variation (CV).

Statistical data analysis

Microsoft Excel 2016, GraphPad Prism 8.3.0 (La Jolla, CA) and R 3.6.0 were used for statistical analysis. Data were presented as mean and SD, when a measure of (interindividual) variability was required, or SEM to describe an error in laboratory procedures. CV was used to describe variability. Multivariate analyses (hierarchical cluster analysis and principal components analysis) were used to assess global differences in gene expression. Pearson's correlation (r) was used to assess RNA-protein correlations in matched samples, and scatter around a linear fit was assessed by linear regression (R^2). Differences between

patients and controls were tested using unpaired *t*-test with Welch's correction for dissimilar variance. Effects of demographics on expression and shedding were assessed using unpaired *t*-test for differences between male and female donors and linear regression for associations with age and body mass index. A cutoff *P* value of 0.05 was used for significance (Bonferroni-corrected for multiple iterations). Receiver operator characteristic (ROC) analysis was performed for liquid biopsy measurements against tissue levels (used as a reference); the area under the ROC curve (AUC) was used to assess the predictive value of the test.

RESULTS

Plasma exosomal transcriptome

Plasma cfRNA from 29 patients with cancer and 5 healthy donors was extracted and sequenced (**Figure 1a**). Exosomes were first isolated and examined by electron microscopy (**Figure 1b**), reflecting a size range of 30–100 nm. Exosomal cfRNA was then extracted and its quality and yield were assessed. The RNA quality parameter DV200 was 47% ± 24% for the patient set (and 64% ± 9% in healthy controls). DV200 < 15% was recorded following exosomal lysis, confirming the protective role of vesicles against RNA degradation. RNA concentration in patient samples was 1.2 ± 0.8 ng/μL (0.4–3 ng/μL; **Figure 1c**), translating to a yield of 7.3 ± 4.4 ng/mL plasma, compared with 1.8 ± 0.5 ng/mL from healthy plasma. The cDNA concentration ranged from 2.1 to 12.8 ng/μL in the patient set (**Figure 1c**), compared with 0.6–5.1 ng/μL in controls.

AmpliSeq achieved highly multiplexed targeted sequencing of > 20,000 human RefSeq[26] genes in a single assay, generating a set of reads for each sample (each read is a data string of bases corresponding to each targeted cDNA fragment from each transcript). The number of reads mapped to a certain transcript was used as quantitative output. In total, 47–137 million reads were recorded in plasma from patients compared with 42–96 million in healthy plasma. Sequencing quality was excellent, with 97.3% of sequenced bases in the patient set (and 93.9% in the healthy set) achieving quality scores (Q-scores) of ≥ 30; i.e., ≥ 99.9% base call accuracy (**Figure 1d**). The number of transcripts measured in patient samples ranged from 18,128 to 21,334, compared with 17,869–19,816 in the healthy set. Technical variability in healthy samples (**Figure S1**) reflected high global reproducibility across replicates. Comparison of the expression of > 20,000 genes between healthy and patient plasma by multivariate analysis showed clear distinction between the two sets (**Figure S2**). A total of 171 and 362 gene transcripts of drug/xenobiotic-metabolizing enzymes and transporters (**Tables S3** and **S4**), respectively, were quantifiable in plasma. Of these, 89 enzymes and 71 transporters were liver enriched.

Variability in liver-to-blood exosomal shedding

Liver-specific markers and targets (enzymes/transporters) are constitutively expressed in the liver and released within exosomes at variable rates in different patients (**Figure 2a**). Variability in blood measurements combines variability in tissue expression and variability in shedding. Shedding was described using a novel parameter (SF) constructed using 13 liver-specific

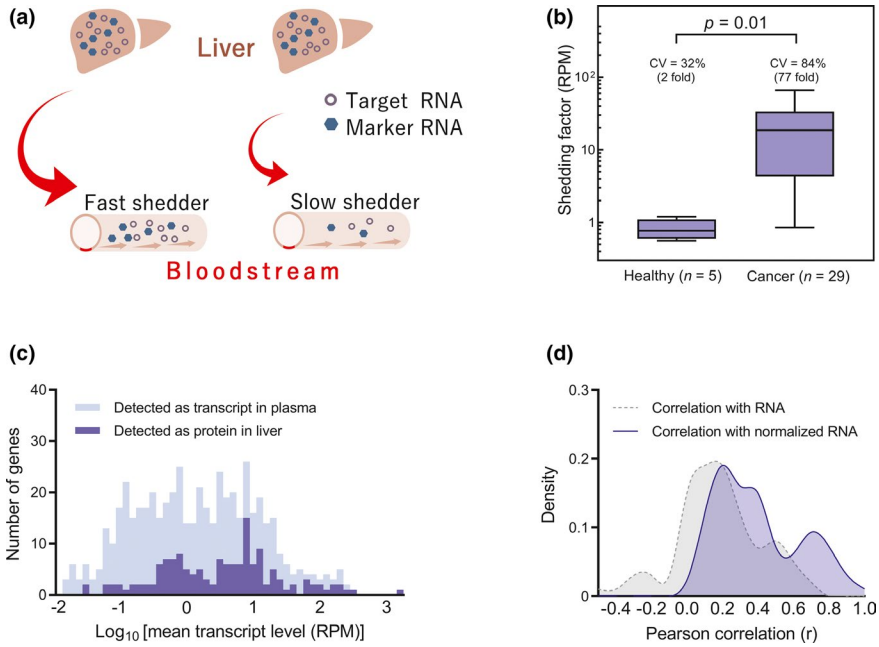

Figure 2 Exosomal RNA shedding from the liver to the bloodstream. (**a**) Markers specific to the liver and targets are expressed in the liver and released in exosomes at different rates in different patients; variability in measured targets in the bloodstream comprises variability in expression and variability in shedding. (**b**) Measurement of shedding variability using 13 markers (**Table1**) revealed higher and more variable shedding from the liver in patients with cancer compared with healthy controls; *P* = 0.01. The whiskers represent the range, boxes represent the 25th and 75th centiles, and the lines are the medians. (**c**) Pharmacologically relevant target genes showed evidence of expression and shedding into the bloodstream (533 transcripts) and evidence of expression as protein in liver tissue (147 proteins). (**d**) Correlation between liver-enriched proteins and their corresponding RNA transcripts in plasma (97 targets) improved by normalization of RNA levels for shedding. RPM, reads per million.

markers[27] measured in plasma exosomes (**Table S5**). SF variability and reproducibility across two technological platforms (Ion Proton by Thermo and NovaSeq by Illumina) are shown in **Figure S3**. SF levels in the patient and healthy sets was 22.16 ± 18.57 RPM (CV 84%) and 0.83 ± 0.26 RPM (CV 32%), respectively (**Figure 2b**). This reflects shedding 26-fold higher and 2.6-fold more variable in patients with cancer relative to healthy controls ($P = 0.01$). There were no significant differences in shedding between male and female donors ($P > 0.05$) and no significant association with age or body mass index ($P > 0.05$).

Hepatic membrane proteome

Membrane fractions were extracted from liver samples (matching the cancer plasma set). Membrane protein content per gram liver was 10.16 ± 5.07 mg/g. Recovery of reticular membrane (relevant to enzymes) and plasma membrane (relevant to transporters) was 70.2% ± 7.7% and 54.5% ± 28.1%, respectively (**Figure 1e**). Global proteomic analysis of membrane fractions identified a total of 12,331 peptides (8,417 ± 503 per sample) and 2,562 proteins (1,578 ± 91 per sample), with an average of 5 peptides per protein (**Figure 1f,g**). Of the identified proteins, 2,143 proteins, spanning 5 orders of magnitude, were quantified (**Figure 1h**). Reliable quantification of a protein was considered when (a) there was evidence of its expression in liver (Human Protein Atlas),[28] (b) it was identified by at least one unique or razor peptide, and (c) it was quantified in > 10% of individual and quality control samples. More than 95% of the quantified proteins were mapped to a membrane compartment, constituting 91% of total membrane protein mass (**Figure S4a,b**). Quantified proteins were predominantly reticular, nuclear, mitochondrial, or cell membrane proteins; there was small contamination from cytoskeletal proteins (13% by mass).

Functional annotation revealed that 588 quantified proteins had enzymatic activity and 377 played a role in transport. These included 88 enzymes and 59 transporters involved in pharmacology. Enzymes included 22 cytochrome P450 proteins and 11 uridine-5'-diphospho-glucuronosyltransferases, and transporters included 14 ATP-binding cassette transporters and 45 solute carriers (**Figure S4c**). Targeted analysis focused on key enzymes and transporters quantifiable by in-house QconCAT standards and the list was refined using predefined criteria (**Table 1**). Abundance of the selected targets (12 enzymes and 4 transporters) was measured in enriched membrane fractions (**Table S7**) and scaled up to specific content in tissue (**Table S8**). Overall, the abundance values were in agreement with recent meta-analyses.[29–31]

Correlation between plasma transcript and hepatic protein levels

Expression of pharmacologically relevant genes was demonstrated in plasma at the RNA level (533 genes) and in liver tissue at the protein level (147 genes; **Figure 2c**). Correlations between plasma RNA and tissue protein measurements were improved for liver-enriched genes (97 genes) upon normalization to liver shedding by at least + 0.2 in Pearson's coefficient (r) (**Figure 2d**). As a proof of principle, RNA (normalized for shedding) and protein expression data for 12 key drug-metabolizing enzymes and 4 drug transporters are summarized in **Figure 3a,b**. Individual values are listed in **Tables S6** and **S8**, respectively. Significant relationships were demonstrated for these genes in 29 matched samples (**Figure 3c**). Notably, correlations were strongest and most significant for cytochrome P450 enzymes ($r = 0.70–0.87$, $P < 0.001$, $R^2 = 0.50–0.75$), compared with glucuronosyltransferases ($r = 0.60–0.80$, $P < 0.05$, $R^2 = 0.36–0.65$) and transporters ($r = 0.66–0.74$, $P < 0.01$, $R^2 = 0.43–0.54$; **Table S9**). These correlations are a dramatic improvement over correlations prior to normalization (cytochrome P450 enzymes ($R^2 = 0.00–0.53$), glucuronosyltransferases ($R^2 = 0.00–0.52$), and transporters ($R^2 = 0.04–0.21$)).

Liquid biopsy measurement as a test for patient stratification

To assess the utility of the developed test in patient stratification, ROC analysis was applied to data for six P450 enzymes (CYP3A4, 2D6, 2C9, 1A2, 2A6, and 2C19), four glucuronosyltransferases (UGT1A1, 1A9, 2B4, and 2B7), and four transporters (P-gp, BCRP, MRP2, and OATP1B1) in order to identify the top and bottom quartiles of the patient set. The two quartiles reflect extremes of drug exposure; the top quartile represents patients susceptible to lack of efficacy, and the bottom quartile represents patients most likely to experience toxicity. The test was effective as a predictor of the bottom quartile (AUC ≥ 0.64; **Figure 4a**) and performed even better with the top quartile (AUC ≥ 0.77; **Figure 4b**). Predictions for P450 enzymes were better than predictions for transferases and transporters. Identification of the extremes in population distribution of drug exposure can inform dose adjustment, whereas the middle group usually require a standard dose of the drug (**Figure 4c**).

Simulated drug exposure with liquid biopsy guided dose adjustment

Exposure (AUC of the plasma concentration-time profile) to three CYP3A substrates (alprazolam, midazolam, and ibrutinib) was simulated with dosing adjusted based on either stratified (**Figure 5a**) or individualized (**Figure 5b**) regimens. The outcome was compared with a uniform oral dose. Simulations demonstrated similar average drug exposure with significant reduction in variability with stratified and individualized dosing (**Figure 5c**). Stratification led to 1.7-fold reduction in variability in all cases, whereas individualized dosing resulted in further reduction from 50% to 25% (2-fold), 84% to 42% (2- fold), and 76% to 31% (2.5-fold) for alprazolam, midazolam, and ibrutinib, respectively (**Figure 5d**). The reduced variability in exposure reflects improved precision of oral dose selection.

DISCUSSION

In this study, we present data in support of a novel pharmacological test for characterizing hepatic elimination capacity in individual patients by means of a "liquid biopsy." The test is a minimally invasive method for the identification of patients susceptible to toxicity due to overdosing and those prone to ineffective therapy

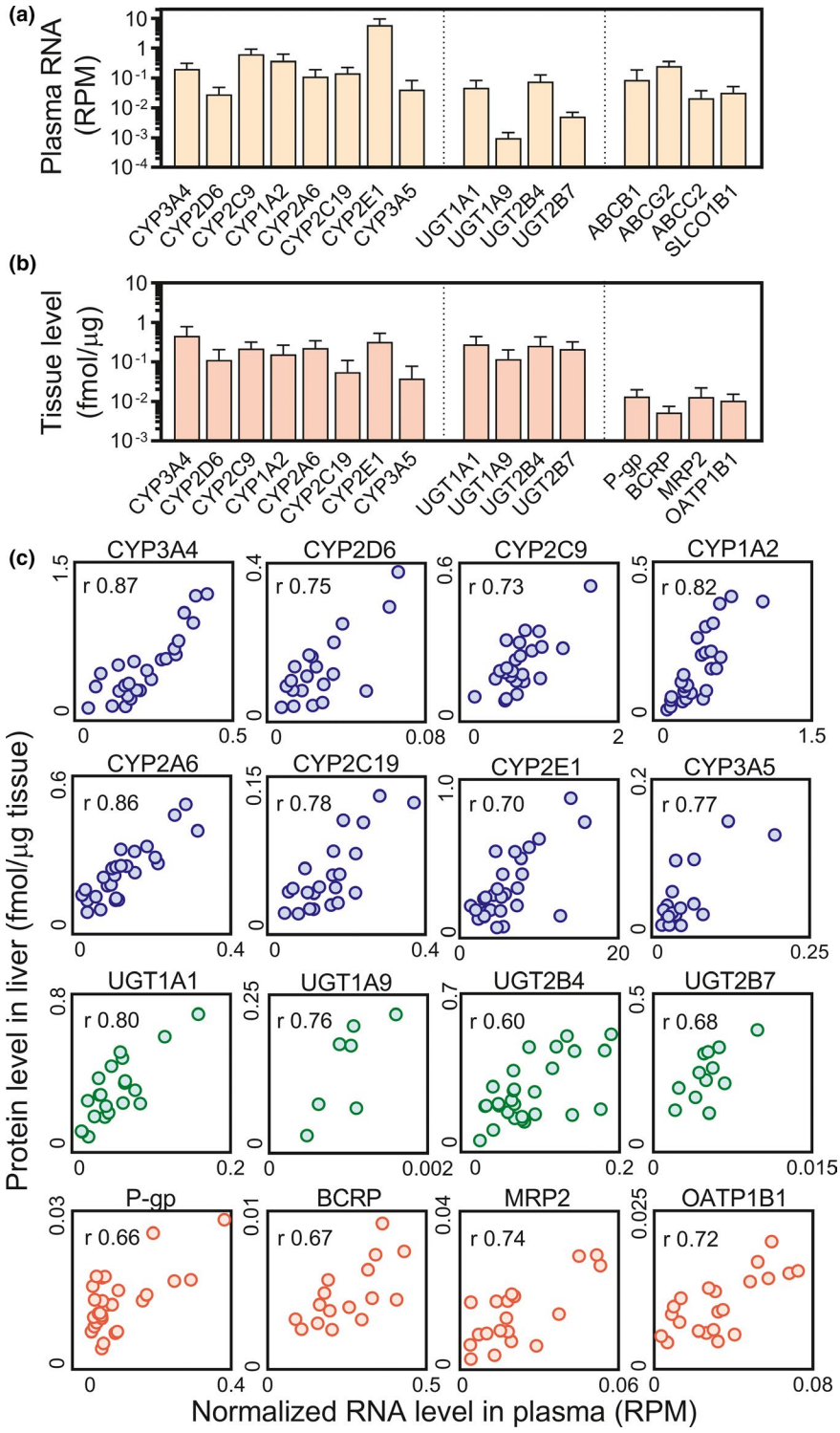

Figure 3 Linking plasma measurements to liver content of enzymes and transporters. (**a**) Plasma RNA levels were normalized to individual shedding. (**b**) Protein levels were measured in unit tissue mass. Levels are presented as means ± SD. (**c**) Correlation matrix showing a quantitative link between the levels in plasma and liver tissue. Pearson's correlation coefficients (*r*) were in the ranges 0.70–0.87 ($P < 0.001$), 0.60–0.80 ($P < 0.05$), and 0.66–0.74 ($P < 0.01$) for cytochrome P450 enzymes (blue symbols), transferases (green symbols), and transporters (red symbols), respectively. RNA and protein data represent measurements above the limit of quantification. Plasma levels are expressed in reads per million (RPM) for transcripts measured by sequencing, and tissue levels are expressed in femtomoles of target protein per microgram liver tissue measured by targeted proteomics.

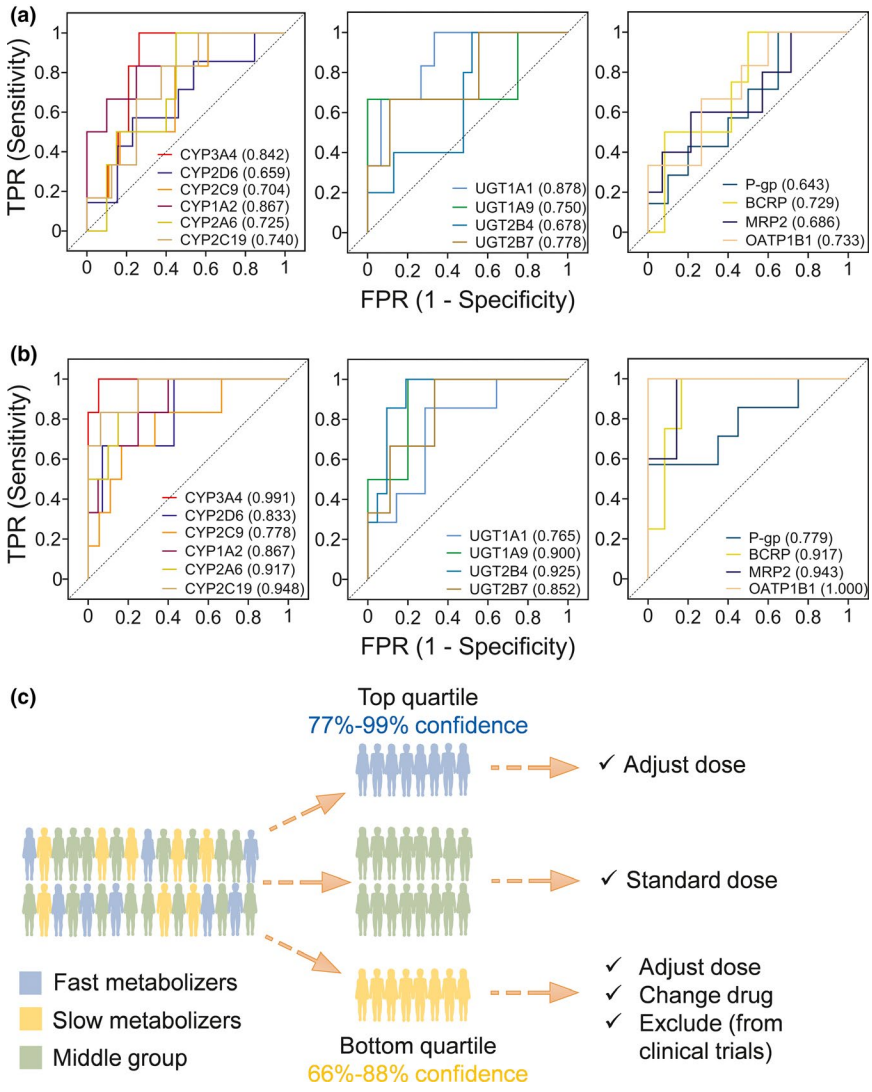

Figure 4 The use of liquid biopsy test for patient stratification. (**a**) Receiver operator characteristic (ROC) analysis of the liquid biopsy test for predicting the bottom quartile of the patient set. (**b**) ROC analysis for the identification of the top quartile. The test was applied with data for six hepatic P450 enzymes (CYP3A4, 2D6, 2C9, 1A2, 2A6, and 2C19), four glucuronosyltransferases (UGT1A1, 1A9, 2B4, and 2B7), three efflux transporters (P-gp, BCRP, and MRP2), and one uptake transporter (OATP1B1). TPR and FPR represent true and false positive rates, respectively, the dashed diagonal line represents random chance, and area under the curve (AUC) values are shown in parentheses. Predictions of the bottom quartile were accurate (AUC ≥ 0.64) and those of the top quartile were very accurate (AUC ≥ 0.77). Predictions for P450 enzymes were better than predictions for transferases and transporters. (**c**) Stratification of patients to identify slow metabolizers (bottom quartile) and fast metabolizers (top quartile) in relation to key drug-metabolizing enzymes. The top quartile is likely to receive ineffective dosing whereas the bottom quartile is likely to experience toxicity. The prediction of patient strata facilitates decision making in relation to dose adjustment and choice of drug.

due to underdosing. Because the test is not drug-specific, it has the advantage over traditional therapeutic drug monitoring of being applicable to all drug substrates of the quantified enzymes and transporters. Clinical use of liquid biopsy has so far focused on diagnostics, especially in oncology,[32] and we propose that the developed test will address the gap in therapeutic applications, which have only recently started to be explored.[33,34]

Implementation of the assay relies on quantitative characterization of clinically relevant enzymes and transporters in plasma exosomes. Exosomes are small extracellular vesicles (30–100 nm in size),[35] released by tissues into the bloodstream at different rates, depending on physiological conditions, disease states, and medication. Exosomes enclose proteins and nucleic acids sampled from the intracellular biomolecular pool.[33,36] We focused on enzymes and transporters that play a key role in determining the level of administered drug that reaches the systemic circulation. Remarkably, cfRNA screening revealed, for the first time, the presence of a wide range of pharmacologically relevant enzymes (171 transcripts) and transporters (362 transcripts) in plasma exosomes, which were readily quantifiable. Of these, 160 targets were liver enriched and may therefore be used to monitor liver activity. Proteomic evidence showed that 28% (i.e., 147) of the 533 pharmacologically relevant genes quantified as transcripts in plasma were detectable as corresponding proteins in liver tissue. These

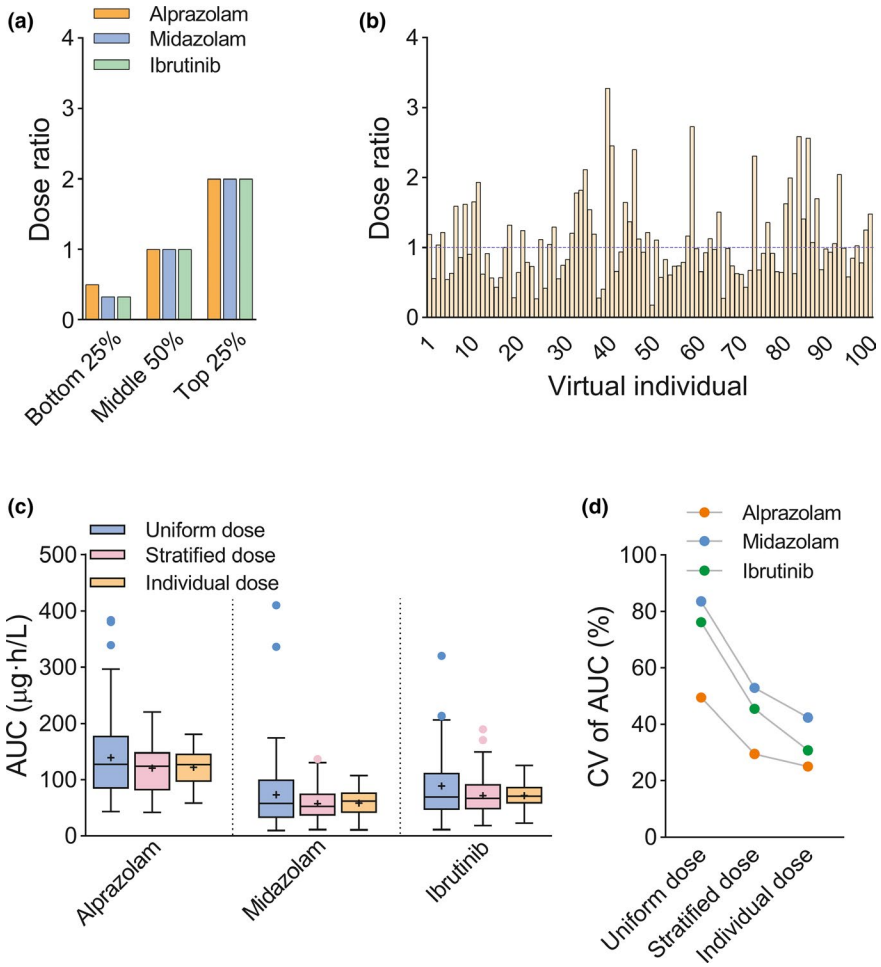

Figure 5 *In silico* drug trials with liquid biopsy technology for alprazolam, midazolam, and ibrutinib following uniform, stratified, or individualized dosing. (**a**) Stratified dosing relied on a dose ratio for each of three groups of patients (top quartile, bottom quartile, and middle 50%) relative to a uniform dose of alprazolam (0.5 mg), midazolam (5 mg), and ibrutinib (140 mg). (**b**) Individualized dosing was performed based on individual dosage adjustment using patient-specific ratios relative to the defined uniform dose. The dose adjustment ratios in all cases were informed by liquid biopsy measurements, and the dose was calculated as the selected ratio multiplied by the uniform dose. (**c**) Simulation of the level of drug exposure (area under the curve (AUC) of the plasma concentration-time profile) after an oral dose of the three drugs; similar levels of the drug reached the systemic circulation over time in the three dosing scenarios. The whiskers represent the range of AUC, boxes represent the 25th and 75th centiles, the lines are the medians, and the + signs are the means. (**d**) Reduction in variability in exposure following stratified and individualized dosing informed by liquid biopsy was observed in all cases.

genes are generally expressed at low levels, and transcriptomic analysis has the advantage of amplification of cDNA, allowing better detection.

A quantitative link between liquid biopsy and tissue measurements was required for the test. Variability in plasma transcript levels comprises variability in liver expression and variability in shedding from the liver into the bloodstream. Liver-specific shedding was described quantitatively by a novel parameter (SF), which comprises quantitative RNA input for 13 markers. Liver shedding was found to be higher and more variable in patients with liver cancer than healthy controls. A similar trend of elevated levels of circulating exosomes was previously demonstrated for ovarian,[37] oesophageal,[38] colorectal,[39] and hematological[40] cancer. Normalization for shedding improved correlation between liver protein and plasma transcript levels for liver-enriched genes, leading to strong and significant correlations for P450 enzymes and moderate to strong correlations for transferases and transporters. Differences in shedding between the healthy and cancer sets indicate that implementation of shedding normalization is likely to be population and disease-specific. Previous studies reported the presence of a limited number of P450 enzymes (12 targets) and glucuronosyltransferases (10 targets) in exosomes isolated from human plasma[33,41]; quantitative analysis demonstrated correlation for only one enzyme (CYP3A4) against specific liver activity (midazolam).[33] Attempts to identify enzymes in urine exosomes have not been successful[42] and no previous work reported measurement of transporters in a liquid biopsy.

Correlation between RNA and protein in tissue has been investigated previously, often with conflicting outcomes.[43–45] RNA measurements normally capture a "snapshot" of the dynamic levels of transcripts in cells, which can go up or down depending on their specific turnover. More rigorous studies have shown better correlations than previously thought, especially for transcripts

and proteins with relatively slow turnover (longer half-lives).[43,46] The strong correlations shown in the present study could be due to the continuous shedding of RNA within exosomes into the bloodstream, where the levels in the pool (plasma) do not fluctuate as much as tissue levels. This theory is consistent with an expected "damping effect," resulting in measurement of steady-state (time-averaged) RNA levels in plasma.

Recent reports[15,34] outlined the necessary requirements and expected trajectory to the application of liquid biopsy techniques in drug development and clinical practice. Proposed applications include patient stratification to achieve more precise dosing and improved characterization of volunteers prior to enrollment in clinical trials. The requirement for changing a dosage regimen in these applications is highlighted in cases of adverse drug reactions or when a recommended dose is ineffective. Toxicity cases are associated with high levels of exposure to the drug, whereas cases of ineffective dosing are characterized by low exposure. We assessed the developed test as a tool to identify patients at the extremes of drug exposure (top and bottom quartiles). Accurate predictions were achieved for both groups, especially in the case of P450 enzymes. Taking the main drug-metabolizing enzyme, CYP3A4, as an example, the test identified the top quartile at 99% confidence and the bottom quartile at 84% confidence. Simulated trials of three CYP3A substrates (alprazolam, midazolam, and ibrutinib) demonstrated reduced variability in exposure (by 2-fold–2.5-fold) following oral dose adjustment using liquid biopsy input. The reduced variability in predicted drug exposure suggests that a more precise dose selection can be made in advance of initiating therapy using such technology.

In conclusion, this study demonstrates quantitative liquid biopsy projections based on plasma measurements to determine liver content of key enzymes and transporters. Considering the importance of intestinal and renal elimination, extension of this work to the attributes of the gut and kidneys is a necessary step for successful application in the clinical setting. Integration of this technique with specific pharmacokinetic models should facilitate efforts toward delivering precise and effective dosage regimens (precision dosing), as an essential element of precision medicine. Limitations of the developed technology include its high cost (which is expected to go down as technology improves and becomes more wide spread), the requirement for specialist expertise in exosomal isolation and multi-omics (which we envisage might become more automated), and most importantly the need for verification of the quantitative link between liquid biopsy and tissue in wider patient groups and repeated samples from the same individuals (which will be accumulated over time as other investigators apply the technique in their own settings).

SUPPORTING INFORMATION

Supplementary information accompanies this paper on the *Clinical Pharmacology & Therapeutics* website (www.cpt-journal.com).

ACKNOWLEDGMENTS

The authors would like to thank Professor James E. Rothman of Yale University for instructive consultations in relation to the direction of the study. We also thank the Manchester Biomedical Research Centre (BRC) Biobank, University of Manchester, for access to matched patient samples, the Biological Mass Spectrometry Core Facility (BioMS), University of Manchester, for access to liquid chromatography coupled to mass spectrometry instrumentation and the Electron Microscopy Core Facility, University of Manchester, for access to transmission electron microscopy.

FUNDING

This work was funded by Certara Ltd., Princeton, NJ, USA.

CONFLICT OF INTEREST

A.G.-G. is an employee of Illumina. K.L. and J.S. are employees of Thermo Fisher Scientific. P.K., M.Z., and A.R.-H. are employees of Certara. All other authors declared no competing interests for this work.

AUTHOR CONTRIBUTIONS

B.A. and A.R.-H. wrote the manuscript. B.A. and A.R.-H. designed the research. B.A., Z.M.A., A.G.-G., K.L., P.K., M.Z., and D.K., performed the research. B.A., Z.M.A., A.G.-G., K.L., J.B., and J.S. analyzed the data.

1. Rawlins, M.D. Variability in response to drugs. *BMJ* **4**, 91–94 (1974).
2. Polasek, T.M. *et al*. What does it take to make model-informed precision dosing common practice? Report from the 1st Asian symposium on precision dosing. *AAPS J.* **21**, 17 (2019).
3. Shahin, M.H. *et al*. The patient-centered future of clinical pharmacology. *Clin. Pharmacol. Ther.* **107**, 72–75 (2020).
4. Venkatakrishnan, K. *et al*. Toward progress in quantitative translational medicine: a call to action. *Clin. Pharmacol. Ther.* **107**, 85–88 (2020).
5. Auffray, C. *et al*. From genomic medicine to precision medicine: highlights of 2015. *Genome Med.* **8**, 12 (2016).
6. Gaedigk, A. *et al*. The CYP2D6 activity score: translating genotype information into a qualitative measure of phenotype. *Clin. Pharmacol. Ther.* **83**, 234–242 (2008).
7. International Warfarin Pharmacogenetics Consortium Estimation of the warfarin dose with clinical and pharmacogenetic data. *N. Engl. J. Med.* **360**, 753–764 (2009).
8. Barber, J., Russell, M.R., Rostami-Hodjegan, A. & Achour, B. Characterization of CYP2B6 K262R allelic variants by quantitative allele-specific proteomics using a QconCAT standard. *J. Pharm. Biomed. Anal.* **178**, 112901 (2020).
9. Ingelman-Sundberg, M. Pharmacogenetics of cytochrome P450 and its applications in drug therapy: the past, present and future. *Trends Pharmacol. Sci.* **25**, 193–200 (2004).
10. Wienkers, L.C. & Heath, T.G. Predicting in vivo drug interactions from in vitro drug discovery data. *Nat. Rev. Drug Discov.* **4**, 825–833 (2005).
11. Cerny, M.A. Prevalence of non-cytochrome P450-mediated metabolism in Food and Drug Administration-approved oral and intravenous drugs: 2006–2015. *Drug Metab. Dispos.* **44**, 1246–1252 (2016).
12. Zhang, L., Zhang, Y. & Huang, S.-M. Scientific and regulatory perspectives on metabolizing enzyme–transporter interplay and its role in drug interactions: challenges in predicting drug interactions. *Mol. Pharm.* **6**, 1766–1774 (2009).
13. Polasek, T.M., Shakib, S. & Rostami-Hodjegan, A. Precision dosing in clinical medicine: present and future. *Expert Rev. Clin. Pharmacol.* **11**, 743–746 (2018).
14. Prasad, B. *et al*. Toward a consensus on applying quantitative liquid chromatography-tandem mass spectrometry proteomics

in translational pharmacology research: a white paper. *Clin. Pharmacol. Ther.* **106**, 525–543 (2019).
15. Darwich, A.S. *et al*. Model-informed precision dosing: Background, requirements, validation, implementation and forward trajectory of individualizing drug therapy. *Annu. Rev. Pharmacol. Toxicol.* https://doi.org/10.1146/annurev-pharmtox-033020-113257.
16. Love, M.I., Huber, W. & Anders, S. Moderated estimation of fold change and dispersion for RNA-seq data with DESeq2. *Genome Biol.* **15**, 550 (2014).
17. Wiśniewski, J.R., Zougman, A., Nagaraj, N. & Mann, M. Universal sample preparation method for proteome analysis. *Nat. Methods* **6**, 359–362 (2009).
18. Feteisi, H.A. *et al*. Identification and quantification of blood-brain barrier transporters in isolated rat brain microvessels. *J. Neurochem.* **146**, 670–685 (2018).
19. Russell, M.R. *et al*. Alternative fusion protein strategies to express recalcitrant QconCAT proteins for quantitative proteomics of human drug metabolizing enzymes and transporters. *J. Proteome Res.* **12**, 5934–5942 (2013).
20. Achour, B., Russell, M.R., Barber, J. & Rostami-Hodjegan, A. Simultaneous quantification of the abundance of several cytochrome P450 and uridine 5′-diphospho-glucuronosyltransferase enzymes in human liver microsomes using multiplexed targeted proteomics. *Drug Metab. Dispos.* **42**, 500–510 (2014).
21. Wiśniewski, J.R. & Rakus, D. Multi-enzyme digestion FASP and the 'total protein approach'-based absolute quantification of the Escherichia coli proteome. *J. Proteomics* **109**, 322–331 (2014).
22. The Uniprot Consortium <https://www.uniprot.org/>. Accessed May 22, 2020.
23. The Gene Ontology Consortium <http://geneontology.org/>. Accessed May 22, 2020.
24. Protein analysis through evolutionary relationships <http://www.pantherdb.org/>. Accessed May 22, 2020.
25. Database for Annotation Visualization and Integrated Discovery <https://david.ncifcrf.gov/>. Accessed May 22, 2020.
26. O'Leary, N.A. *et al*. Reference sequence (RefSeq) database at NCBI: Current status, taxonomic expansion, and functional annotation. *Nucleic Acids Res.* **44**, D733–D745 (2016).
27. Rostami-Hodjegan, A., Achour, B. & Rothman, J.E.Methods and apparatus for quantifying protein abundance in tissues via cell free ribonucleic acids in liquid biopsy. US patent WO 2019/191297 A1 (2019).
28. The Human Protein Atlas <https://www.proteinatlas.org/>. Accessed May 22, 2020.
29. Achour, B., Barber, J. & Rostami-Hodjegan, A. Expression of hepatic drug-metabolizing cytochrome P450 enzymes and their intercorrelations: a meta-analysis. *Drug Metab. Dispos.* **42**, 1349–1356 (2014).
30. Achour, B., Rostami-Hodjegan, A. & Barber, J. Protein expression of various hepatic uridine 5'-diphosphate glucuronosyltransferase (UGT) enzymes and their inter-correlations: a meta-analysis. *Biopharm. Drug Dispos.* **34**, 353–361 (2014).
31. Burt, H.J. *et al*. Abundance of hepatic transporters in Caucasians: a meta-analysis. *Drug Metab. Dispos.* **44**, 1550–1561 (2016).
32. Lanman, R.B. *et al*. Analytical and clinical validation of a digital sequencing panel for quantitative, highly accurate evaluation of cell-free circulating tumor DNA. *PLoS One* **10**, e0140712 (2015).
33. Rowland, A. *et al*. Plasma extracellular nanovesicle (exosome)-derived biomarkers for drug metabolism pathways: a novel approach to characterize variability in drug exposure. *Br. J. Clin. Pharmacol.* **85**, 216–226 (2019).
34. Rodrigues, D. & Rowland, A. From endogenous compounds as biomarkers to plasma-derived nanovesicles as liquid biopsy; has the golden age of translational pharmacokinetics-absorption, distribution, metabolism, excretion-drug–drug interaction science finally arrived? *Clin. Pharmacol. Ther.* **105**, 1407–1420 (2019).
35. Colombo, M. *et al*. Analysis of ESCRT functions in exosome biogenesis, composition and secretion highlights the heterogeneity of extracellular vesicles. *J. Cell Sci.* **126**, 5553–5565 (2013).
36. Max, K.E.A. *et al*. Human plasma and serum extracellular small RNA reference profiles and their clinical utility. *Proc. Natl. Acad. Sci.* **115**, E5334–E5343 (2018).
37. Taylor, D.D. & Gercel-Taylor, C. MicroRNA signatures of tumor-derived exosomes as diagnostic biomarkers of ovarian cancer. *Gynecol. Oncol.* **110**, 13–21 (2008).
38. Matsumoto, Y. *et al*. Quantification of plasma exosome is a potential prognostic marker for esophageal squamous cell carcinoma. *Oncol. Rep.* **36**, 2535–2543 (2016).
39. Silva, J. *et al*. Analysis of exosome release and its prognostic value in human colorectal cancer. *Genes Chromosomes Cancer* **51**, 409–418 (2012).
40. De-Luca, L. *et al*. Characterization and prognostic relevance of circulating microvesicles in chronic lymphocytic leukemia. *Leukemia Lymphoma* **58**, 1424–1432 (2017).
41. Kumar, S. *et al*. Specific packaging and circulation of cytochromes P450, especially 2E1 isozyme, in human plasma exosomes and their implications in cellular communications. *Biochem. Biophys. Res. Comm.* **491**, 675–680 (2017).
42. Moon, P.-G. *et al*. Proteomic analysis of urinary exosomes from patients of early IgA nephropathy and thin basement membrane nephropathy. *Proteomics* **11**, 2459–2475 (2011).
43. Schwanhüusser, B. *et al*. Global quantification of mammalian gene expression control. *Nature* **473**, 337–342 (2011).
44. Vogel, C. *et al*. Sequence signatures and mRNA concentration can explain two-thirds of protein abundance variation in a human cell line. *Mol. Syst. Biol.* **6**, 400 (2010).
45. Wilhelm, M. *et al*. Mass-spectrometry-based draft of the human proteome. *Nature* **509**, 582–587 (2014).
46. Wang, D. *et al*. A deep proteome and transcriptome abundance atlas of 29 healthy human tissues. *Mol. Syst. Biol.* **15**, e8503 (2019).